Bioorganic Chemistry 90 (2019) 103046

Contents lists available at ScienceDirect

Bioorganic Chemistry

journal homepage: www.elsevier.com/locate/bioorg

# Cytotoxic and neuroprotective activities of constituents from *Alternaria alternate*, a fungal endophyte of *Psidium littorale*

Jian Xu[a], Yun-Wei Hu[b], Wei Qu[a,c], Ming-Hua Chen[e], Liang-Sheng Zhou[f], Qi-Rui Bi[a], Jian-Guang Luo[a], Wen-Yuan Liu[b], Feng Feng[a,c,d,*], Jie Zhang[a,*]

[a] Department of Natural Medicinal Chemistry, School of Traditional Chinese Pharmacy, China Pharmaceutical University, Nanjing 210009, People's Republic of China
[b] Key Laboratory of Drug Quality Control and Pharmacovigilance (China Pharmaceutical University), Ministry of Education, China Pharmaceutical University, Nanjing 210009, People's Republic of China
[c] Key Laboratory of Biomedical Functional Materials, China Pharmaceutical University, Nanjing 211198, People's Republic of China
[d] Jiangsu Food & Pharmaceutical Science College, Huaian 223003, People's Republic of China
[e] NHC Key Laboratory for Microbial Drug Bioengeering, Institute of Medicinal Biotechnology, Chinese Academy of Medical Sciences and Peking Union Medical College, Beijing 100050, People's Republic of China
[f] College of Health Sciences, Jiangsu Normal University, Xuzhou 221116, People's Republic of China

ARTICLE INFO

*Keywords:*
*Alternaria alternate*
Liphatic polyketone
Cytotoxic activity
Neuroprotective activity

ABSTRACT

Chemical investigation of the EtOAc extract of the plant-associated fungus *Alternaria alternate* in rice culture led to the isolation of a novel liphatic polyketone, alternin A (**1**), a new indole alkaloid (**8**), and a new sesquiterpene (**11**), together with 12 known compounds. Their structures were elucidated by the interpretation of extensive spectroscopic data, and the absolute configurations of **1**–**3** were established using calculations of ECD spectra, NMR data, and optical rotation values. Compound **1** possesses an unprecedented C25 liphatic polyketone skeleton. Compounds **5** and **10** exhibited potential cytotoxic activities against MCF-7 and HepG cells, and compounds **2**, **7**, and **9** exhibited potential neuroprotective activities in glutamate induced-PC12 injured cells.

## 1. Introduction

Recently, secondary metabolites from plant-associated fungi have drawn attention from chemists and pharmacologists due to their novel structures and significant biological activities. The genus *Alternaria*, comprising more than 250 species, is widely distributed in the natural environment [1], and some members of this genus exhibit phytotoxicity because of the production of multifarious phytotoxins, such as polyketides [2,3], pyrone derivatives [4], and cyclic depsipeptides [5]. In recent years, many novel secondary metabolites, belonging to different classes of natural products, including aromatic polyketide dimers, dibenzo-α-pyrones, dehydrocurvularins, diterpenoids, cyclic pentadepsipeptides, tricycloalternarenes, and sulochrin dimers, have been reported in the genus *Alternaria* [6–12]. Additionally, some of these molecules display acetylcholinesterase inhibition, neuroprotective, cytotoxic, PPAR-γ antagonistic, IKKβ inhibition, and antibacterial activities [6–11].

*Alternaria alternate*, a common fungus, is widely distributed in plants. However, only several alternariols, nitidasanes, and tricycloalternarenes have been reported from this fungus [12–14]. By analyzing the EtOAc extract of *A. alternate* in rice culture using thin layer chromatography (TLC) and high performance liquid chromatography-electrospray mass spectrometry (HPLC-MS), we found that the extract contained a variety of secondary metabolites. To clarify the active compounds, a systematic chemical investigation of the EtOAc extract of *A. alternate* was performed, which led to the isolation of three new compounds and 12 known compounds. In addition, the neuroprotective and cytotoxic activities of these compounds were evaluated in this paper.

## 2. Experimental section

### 2.1. General experimental procedures

Optical rotations and ECD spectra were obtained on a Perkin-Elmer 341 polarimeter and an Applied Photophysics Chirascan spectrometer, respectively. A Waters Micromass Q-TOF instrument was used to measure HRESIMS data. NMR spectra were acquired on Bruker AM-600, AM-400 and AM-300 spectrometers at 25 °C. Semipreparative HPLC with a SPD-M20A PDA detector was carried out on a YMC-Pack

* Corresponding authors.
*E-mail addresses:* fengsunlight@163.com (F. Feng), cpunmc_zj@163.com (J. Zhang).

https://doi.org/10.1016/j.bioorg.2019.103046
Received 28 April 2019; Received in revised form 5 June 2019; Accepted 5 June 2019
Available online 06 June 2019
0045-2068/ 

**Table 1**
$^{1}H$ and $^{13}C$ NMR data for compound **1–3** in $CDCl_3$ ($\delta$ in ppm, $J$ in Hz).

| Position | **1**[a] | | **8**[b] | | **11**[c] | |
|---|---|---|---|---|---|---|
| | $\delta_H$ | $\delta_C$ | $\delta_H$ | $\delta_C$ | $\delta_H$ | $\delta_C$ |
| 1 | 3.86, s | 72.0 | | | 3.39, t (2.4) | 74.6 |
| 2 | 2.55, m | 42.7 | 7.11, d (2.4) | 123.0 | 1.92, dd (3.0, 5.1) 1.73, overlapped | 31.1 |
| 3 | 1.87, m | 39.2 | | 108.5 | 2.16, ddd (2.1, 5.1, 12.9) 2.37, overlapped | 31.9 |
| 4 | 4.79, dd (8.4, 10.8) | 83.0 | 7.36, d (8.0) | 111.4 | | 147.9 |
| 5 | 5.57, dd (8.4, 15.0) | 128.5 | 7.18, dt (1.2, 7.2) | 119.8 | 2.34, overlapped | 50.5 |
| 6 | 6.29, dd (10.8, 15.0) | 135.0 | 7.23, dt (1.2, 7.2) | 122.3 | 3.72, t (9.6) | 67.4 |
| 7 | 6.11, dd (10.8, 15.0) | 135.3 | 7.65, d (8.0) | 118.6 | 1.31, overlapped | 49.4 |
| 8 | 6.23, dd (10.8, 15.0) | 129.1 | | 136.2 | 1.53, m 1.27, overlapped | 18.0 |
| 9 | 6.04, dd (10.8, 15.0) | 127.9 | | 127.1 | 1.83, overlapped 1.22, overlapped | 33.0 |
| 10 | 5.69, dd (7.2, 15.0) | 142.5 | 3.83, dd (0.4, 14.6) 3.80, dd (0.4, 14.6) | 31.8 | | 42.0 |
| 11 | 2.44, m | 34.9 | | 171.8 | 2.26, m | 25.8 |
| 12 | 2.09, overlapped 1.95, dd (7.8, 8.8) | 47.5 | 4.77, m (6.4) | 75.5 | 0.88, d (6.9) | 16.1 |
| 13 | | 134.3 | 3.71, m (6.4) | 70.1 | 0.96, d (6.9) | 21.3 |
| 14 | 5.77, d (10.8) | 126.8 | 1.11, d (6.4) | 18.9 | 5.02, s 4.73, s | 107.1 |
| 15 | 6.18, dd (10.8, 15.0) | 124.7 | 1.25, d (6.4) | 16.4 | 0.76, s | 17.9 |
| 16 | 5.45, dd (7.8, 15.0) | 138.7 | | | | |
| 17 | 2.09, overlapped | 38.8 | | | | |
| 18 | 1.35, overlapped | 29.9 | | | | |
| 19 | 0.86, t (7.8) | 12.0 | | | | |
| 20 | | 174.4 | | | | |
| 21 | 1.31, d (7.2) | 12.9 | | | | |
| 22 | 1.01, d (6.6) | 13.9 | | | | |
| 23 | 0.96, d (6.6) | 20.4 | | | | |
| 24 | 1.70, s | 16.6 | | | | |
| 25 | 0.99, d (6.6) | 19.6 | | | | |
| NH | | | 8.26, br s | | | |

[a] Recorded at 600 MHz.
[b] Recorded at 400 MHz.
[c] Recorded at 300 MHz.

ODS-A column (250 × 10 mm, S-5 μm, 12 nm) with MeOH-$H_2O$ at the flow rate of 2.5 mL/min. ODS (12 nm, S-50 μm, YMC Co., Ltd.), silica gel (200–300 mesh, Qingdao Haiyang Chemical Co., Ltd.), and MCI gel (CHP20P, 75–150 μm, Mitsubishi Chemical Industries Ltd.) were employed for column chromatography.

### 2.2. Isolation and taxonomic identity of *A. alternate*

The fungal strain *A. alternate* was isolated from the leaves of *Psidium littorale* Raddi collected from Quanzhou, Fujian Province, People's Republic of China, in May 2018. The fungus was identified by morphological studies and by comparing its internal transcribed spacer (TIS) sequences with those of known *A. alternate*. (GenBank accession number MH715974.1). The fungal voucher specimen (number: PLR-2017JX-AA) was deposited at the Department of Natural Medicinal Chemistry, China Pharmaceutical University.

### 2.3. Fermentation

Solid fermentation was carried out in 30 Erlenmeyer flasks (1 L), each containing 140 g of rice and 140 mL of water. After autoclaving the contents at 15 psi for 30 min, each flask was inoculated with 20 mL of seed culture and incubated at 25 °C for 30 d.

### 2.4. Extraction and isolation

The fermented material was extracted with EtOAc three times at room temperature. After the evaporation of the combined aqueous EtOAc extracts *in vacuo*, the crude residue (78.0 g) was separated via silica gel column chromatography (CC) and eluted with petroleum ether (PE)-acetone (0:10 to 5:5) to afford 13 fractions Fr.1-Fr.13.

Fr.4 (4.7 g) was subjected to silica gel CC with step-gradient solvent systems of PE-EtOAc (10:1) to give six subfractions Fr.4.1-Fr.4.6. Fr.4.3 (203.1 mg) was repeatedly purified by semipreparative HPLC to yield **12** (7.2 mg; MeOH-$H_2O$ = 90:10, $t_R$ = 35.7 min), and **13** (11.1 mg; MeOH-$H_2O$ = 90:10, $t_R$ = 31.4 min). Fr.4.4 (130.5 mg) was purified by preparative TLC (PE-EtOAc = 5:1, $R_f$ = 0.6) to afford **9** (30.2 mg). Fr.5 (3.5 g) was separated by silica gel CC (PE-acetone = 15:1) to afford seven subfractions Fr.5.1-Fr.5.7. Fr.5.5 (93.2 mg) was purified by semipreparative HPLC (MeOH-$H_2O$ = 87:13, $t_R$ = 40.7 min) to yield **10** (6.1 mg). Fr.7 (3.5 g) was subjected to chromatography over ODS (MeOH-$H_2O$ = 55:45 to 90:10) to give nine subfractions Fr.7.1-Fr.7.7. Fr.7.6 (117.5 mg) was further purified by semipreparative HPLC (MeOH-$H_2O$ = 75:25, $t_R$ = 36.5 min) to give **1** (43.6 mg). Fr.7.3 (407.3 mg) was separated via silica gel CC (PE-EtOAc = 5:1) to give five subfractions Fr.7.3.1-Fr.7.3.5. Fr.7.3.4 (30.5 mg) and Fr.7.3.5 (47.6 mg) were repeatedly purified by recrystallization and semipreparative HPLC (MeOH-$H_2O$ = 73:27, $t_R$ = 31.1 min) to yield **11** (8.7 mg) and **2** (12.5 mg), respectively. Fr.9 (3.5 g) was chromatographed over MCI gel (MeOH-$H_2O$ = 4:6 to 8:2) to obtain seven subfractions Fr.9.1-Fr.9.7. Fr.9.2 (57.3 mg) was purified by recrystallization to yield **4** (35.8 mg). Fr.9.4 (72.1 mg) was repeatedly purified by semipreparative HPLC to yield **7** (6.7 mg; MeOH-$H_2O$ = 45:55, $t_R$ = 29.3 min) and **8** (9.2 mg; MeOH-$H_2O$ = 50:50, $t_R$ = 26.7 min). Fr.10 (3.0 g) was separated via MCI gel CC (MeOH-$H_2O$ = 30:70 to 80:20) to give eight subfractions Fr.10.1-Fr.10.8, followed by semipreparative HPLC to yield **3** [14.9 mg, from Fr.10.3 (71.2 mg); MeOH-$H_2O$ = 36:64, $t_R$ = 27.9 min], **5** [65.7 mg, from Fr.10.4 (125.8 mg); MeOH-$H_2O$ = 39:61, $t_R$ = 35.9 min], **6** [25.1 mg, from Fr.10.2 (77.1 mg); MeOH-$H_2O$ = 32:68, $t_R$ = 29.7 min], **14** (9.6 mg, from Fr.10.2; MeOH-$H_2O$ = 32:68, $t_R$ = 11.7 min), and **15** (12.4 mg, from Fr.10.2; MeOH-$H_2O$ = 32:68, $t_R$ = 18.3 min).

#### 2.4.1. (1) was a colorless oil with the following properties

[$\alpha$]25 D +114.8 ($c$ 0.30, $CH_2Cl_2$); UV (MeOH) $\lambda_{max}$ (log $\varepsilon$) 258 (4.07); IR (KBr), 3491, 2963, 2925, 1725, 1461, 1380, 1204, and 974 $cm^{-1}$; $^{1}H$ and $^{13}C$ NMR data, see Table 1; HRESIMS $m/z$ 387.2863 $[M+H]^+$ (calcd for $C_{25}H_{39}O_3$, 387.2899).

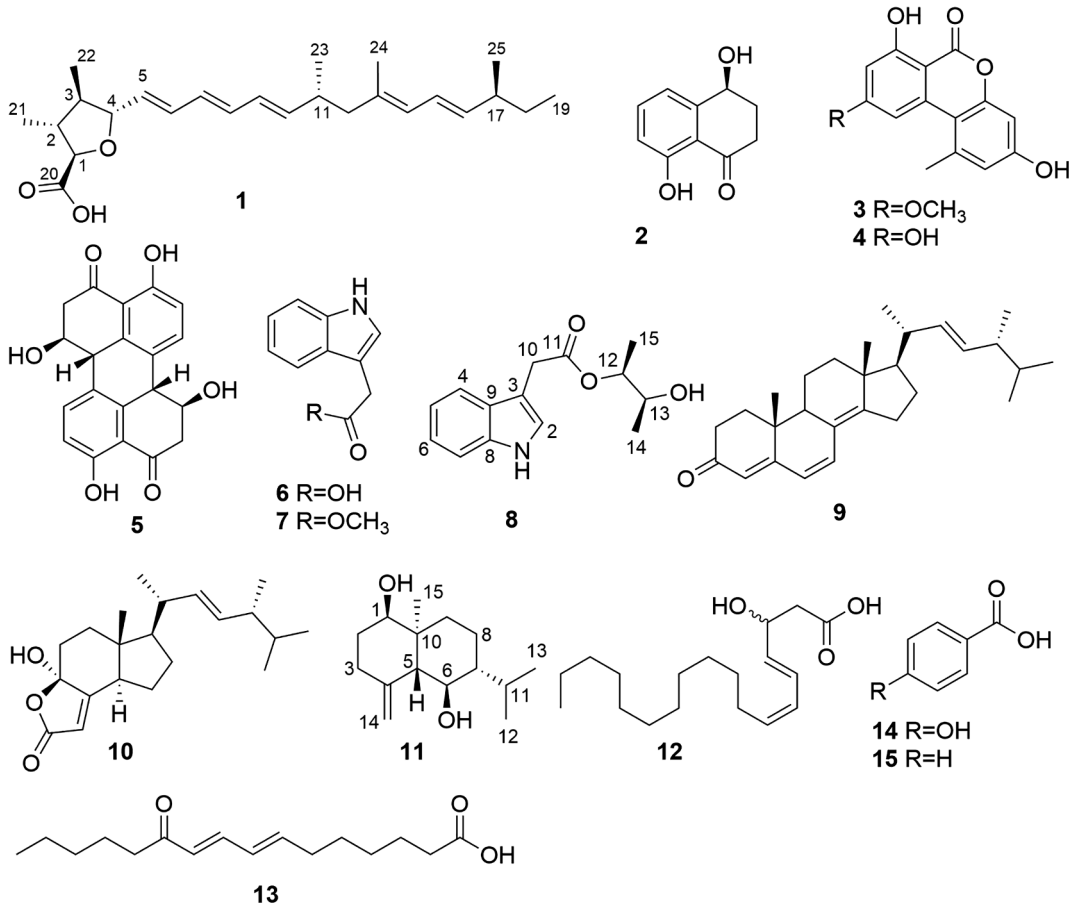


**Fig. 1.** Structures of compounds **1–15**.

*2.4.2. **(8)** was a colorless solid with the following properties*

[α]25 D +52.0 (*c* 0.12, $CH_2Cl_2$); UV (MeOH) $\lambda_{max}$ (log ε) 261 (3.94) nm; IR (KBr), 3267, 2929, 1721, 1445, 1364, 1250, 1179, 1103, 1039, and 743 $cm^{-1}$; $^1H$ and $^{13}C$ NMR data, see Table 1; HRESIMS *m/z* 248.1292 $[M+H]^+$ (calcd for $C_{29}H_{39}O_5$, 248.1287).

*2.4.3. **(11)** was a colorless needle with the following properties;*

[α]25 D −49.5 (*c* 0.20, $CH_2Cl_2$); UV (MeOH) $\lambda_{max}$ (log ε) 215 (3.04) nm; IR (KBr), 3320, 2953, 2928, 1691, 1462, 1381, 1021, and 966 $cm^{-1}$; $^1H$ and $^{13}C$ NMR data, see Table 1; HRESIMS *m/z* 261.1745 $[M+H]^+$ (calcd for $C_{15}H_{27}O_2$, 261.1830).

*2.5. Preparation of the (R)- and (S)-MTPA ester derivatives of **8***

The (*R*)- and (*S*)-MTPA Ester Derivatives of **8** were prepared following the reported procedures [15].

*2.6. Computation methods*

*2.6.1. ECD calculation*

Conformational analysis was carried out via Monte Carlo searching with the MMFF94 molecular mechanics force field using the Spartan 10 software, which afforded stable conformers with an energy cutoff of 2 kcal/mol to the global minima [16]. All these conformers were further optimized using the time-dependent theory (TD-DFT) methodology at the B3LYP/6-31 g(d,p) level in gas phase by using Gaussian09 software [17]. The ECD spectra were calculated using the TD-DFT at the B3LYP/6-31(d,p) level in gas phase [18].

*2.6.2. NMR calculation*

The NMR data of the stable conformers and TMS were calculated using the Gauge-Independent Atomic Orbital (GIAO) method in Gaussian 09 software at the MPWIPW91/6-311 + g(d,p) level. The calculated NMR data of these conformers were averaged according to the Boltzmann distribution theory and their relative Gibbs free energy [19–21].

*2.6.3. Optical rotation calculation.*

The optical rotation (OR) values of the stable conformers were calculated using the TD-DFT at the B3LYP/6-31(d,p) level in $CDCl_3$ by using Gaussian09 software [19–21].

*2.7. Cytotoxicity assays*

The cytotoxic activities of the isolated compounds were determined on 4T-1, A549, HepG-4, and MCF-7 cell lines. The detail procedures were following the previous literature [22]. Gambogic acid was used as the positive control substance.

*2.8. Neuroprotection assays*

The neuroprotective activities of compounds **1–15** were evaluated with a 15 mM glutamate induced-PC12 injured cell model using the MTT method. Nimodipine (150 μM) was used as the positive control substance. The optical density (OD) values were measured using a microplate reader (Thermo Fisher Scientific Co., Waltham, MA, USA) at 490 nm [23,24].

$$\text{Cell viability (\%)} = (OD_{treated} - OD_{blank}) / (OD_{control} - OD_{blank}) \times 100\%.$$

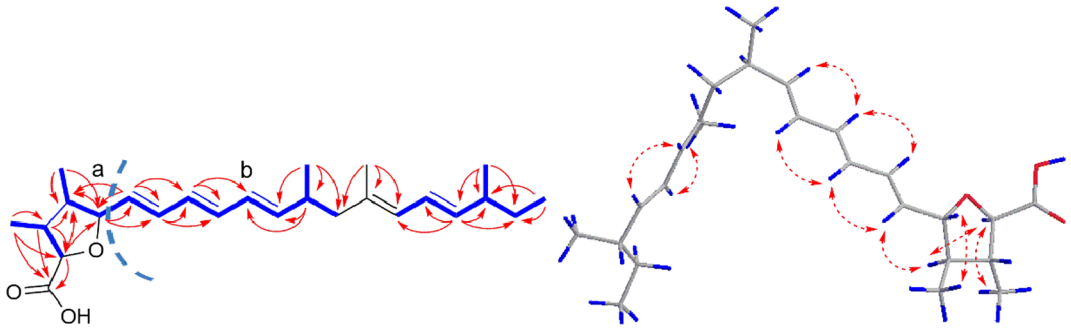


**Fig. 2.** Key $^{1}$H-$^{1}$H COSY (—), HMBC (⤳) and NOESY (⤳) correlations of compound **1**.

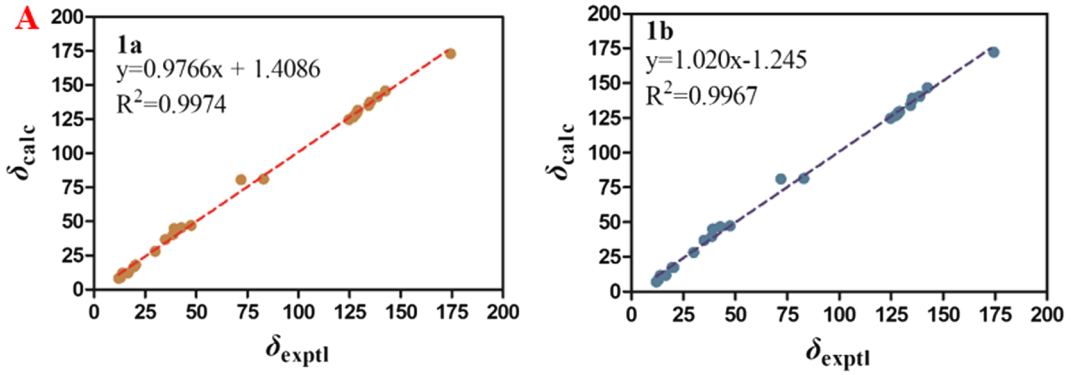


**B**

| DP+ probability of $^{13}$C NMR of **1** | | |
|---|---|---|
| Plausible isomer | **1a** | **1b** |
| sDP4+ | 98.05% | 1.95% |
| uDP4+ | 98.23% | 1.77% |
| DP4+ | 99.96% | 0.04% |

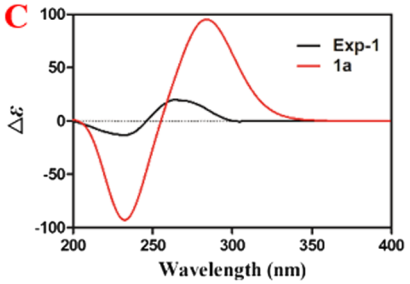


**Fig. 3.** $^{13}$NMR and ECD calculation results of two plausible stereoisomers of **1a**-1*R*,2*R*,3*R*,4*S*,11*R*,17*S* and **1b**-1*S*,2*S*,3*S*,4*R*,11*R*,17*S*. (A) Linear correlation plots of calculated vs experimental $^{13}$C NMR chemical shift values for each potential configuration. (B) The DP4+ probability of chemical shifts. (C) Calculated and experimental ECD spectra of **1**.

## 3. Results and discussion

### 3.1. Isolation of compounds from the EtOAc extract of the rice culture of A. alternate

The EtOAc extract (78.0 g) of the fermentation was isolated and purified by multiple column chromatography on silica gel, MCI, and ODS, preparative TLC, recrystallization, and HPLC to obtain compounds **1–15** (Fig. 1).

### 3.2. Structural elucidation of the isolated compounds

The molecular formula, $C_{25}H_{38}O_3$, of alternin A (**1**) was revealed by the HRESIMS at *m/z* 387.2863 $[M+H]^+$. The 1D NMR spectra of **1** displayed signals for six methyls, two sp$^3$ methylenes, six sp$^3$ methines [including two oxygenated methines at $\delta_H$ 4.79 (dd, $J$ = 8.4, 10.0 Hz) and 3.86 (s), $\delta_C$ 83.0 and 72.0, respectively], nine sp$^2$ methines [$\delta_H$ 5.57 (dd, $J$ = 8.4, 10.8 Hz), 6.29 (dd, $J$ = 10.8, 15.0 Hz), 6.11 (dd, $J$ = 10.8, 15.0 Hz), 6.23 (dd, $J$ = 10.8, 15.0 Hz), 6.04 (dd, $J$ = 10.8, 15.0 Hz), 5.69 (dd, $J$ = 7.2, 15.0 Hz), 5.77 (d, $J$ = 10.8 Hz), 6.18 (dd, $J$ = 10.8, 15.0 Hz), and 5.45 (dd, $J$ = 7.8, 15.0 Hz), $\delta_C$ 128.5, 135.0, 135.3, 129.1, 127.9, 142.5, 126.8, 124.7, and 138.7, respectively], one sp$^2$ quaternary carbon [$\delta_C$ 134.3], and one carbonyl carbon [$\delta_C$ 174.4], as evidenced by HSQC experiments. The comparison of the above data with these of nafuredin A[25] suggested that their structures are closely related, except for the additional signals of a double bond group and a methyl in **1**, indicating **1** was a liphatic polyketone derivative.

The full structure of **1** was established by 2D NMR data analyses (Fig. 2). The $^{1}$H-$^{1}$H COSY correlations of H-4/H-3/H-22, H-2/H-1, and H-21/H-2 and the HMBC correlations from H-22 to C-3 and C-4, from H-21 to C-1 and C-2, from H-2 to C-20, C-1, and C-3, and from H-1 to C-20, C-4, and C-3 confirmed that the additional methyl is located at C-2 in **1**, which allowed to establish the hydrogenated furan moiety (moiety **a**). The methylated olefinic hydrocarbon chain (moiety **b**) with an additional $\triangle^{5,6}$ double bond was indicated by the $^{1}$H-$^{1}$H COSY correlations of H-23/H-11 and H-25/H-17, the contiguous sequence of $^{1}$H-$^{1}$H COSY correlations from H-5 to H-12 and from H-14 to H-19, and the HMBC correlations from H-24 to C-12, C-13, and C-14. Finally, the $^{1}$H-$^{1}$H COSY correlation of H-4/H-5 and the HMBC correlations from H-4 to C-5 and C-6, and from H-5 to C-3 and C-4 allowed the connectivity of moieties **a** and **b** through the C-4—C-5 bond. Thus, the gross structure of **1** was established as shown in Fig. 2.

The geometry of the double bonds in the moiety **b** were all determined to be *E* according to the NOESY correlations of H-5/H-7/H-9, H-24/H-15, and H-16/H-14. Moreover, the comparison of the 1D NMR data of moiety **b** with those of nafuredin A, whose absolute

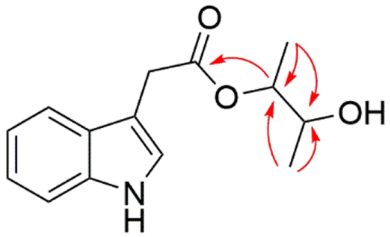


**Fig. 4.** Key HMBC (⟶) correlations of compound **8**.

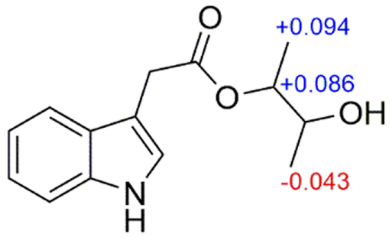


**Fig. 5.** Values of $\Delta\delta(\delta_S–\delta_R)$ (in pyridine-$d_5$) of the MTPA esters of **8**.

configuration was determined based on asymmetric synthesis [25], indicated these molecules shared the same 11*R*,17*S*-configuration. To confirmed the configuration of moiety **a**, the NOESY spectrum was further analyzed. As shown in Fig. 2, the correlations of H-5/H-3/H-1/Me-21 suggested they were all *α*-oriented, while the NOESY cross-peak of H-4/Me-22 revealed their cofacial relationship. Finally, the calculations of the $^{13}$C NMR and ECD data were used for determining the absolute configuration of moiety **a**. [19–21] As shown in Fig. 3, the higher correlation coefficient (**1a**: 0.9974; **1b**: 0.9967) and DP4+ probability (**1a**: 99.96; **1b**: 0.04) between the calculated $^{13}$C NMR data of **1a**-1*R*,2*R*,3*R*,4*S*,11*R*,17*S* and experimental data than these between **1** and **1b**, suggesting **1a** possessed a better agreement with **1** than **1b**. Meanwhile, the calculated ECD spectrum of **1a** was highly similar to the experimental data [18]. Therefore, the absolute configuration of **1** was determined as 1*R*,2*R*,3*R*,4*S*,11*R*,17*S*. Therefore, the structure of **1** was unequivocally characterized as an unprecedented C25 liphatic polyketone skeleton.

The molecular formula, $C_{14}H_{17}NO_3$, of alternatine A (**8**) was determined by HRESIMS. The $^1$H and $^{13}$C NMR spectra of **8** exhibited the characteristic signals of an indole moiety: an NH group ($\delta_H$ 8.26, br s), and five aromatic protons [$\delta_H$ 7.65 (d, $J$ = 8.0 Hz), 7.23 (dt, $J$ = 1.2, 7.2 Hz), 7.18 (dt, $J$ = 1.2, 7.2 Hz), and 7.36 (d, $J$ = 8.0 Hz); $\delta_C$ 118.6, 122.3, 119.8, and 111.4, respectively]. Carefully comparison of the 1D NMR data of **8** with these of compound **6** suggested that they are analogues [26], and the main difference between the two molecules was an additional side chain at C-11 in **8**. The key correlations of $CH_3$-15 with C-12 and C-13, and of $CH_3$-14 with C-12 and C-13 in the HMBC spectrum of **8** (Fig. 4) established the 2,3-butanediol moiety. Moreover, the HMBC correlation of H-12 with C-11 suggested that the 2,3-butanediol moiety was located at C-11 through an ester bond.

Due to the free rotation of the side chain and the non-special coupling constants ($J_{H\text{-}12/H\text{-}13}$ = 6.4 Hz), the relative configurations of C-12 and C-13 were difficult to establish from $^1$H NMR and NOESY spectra. To determine the configuration of C-13, a mosher's method was used. Careful analysis the $^1$H NMR spectra of the (*R*)- and (*S*)-MTPA ester derivatives of **8** (**8r** and **8 s**) revealed the negative chemical shift difference ($\triangle\delta$(*S*-*R*), Fig. 5) for H-14, as well as the positive chemical shift differences for H-15, and H-12, respectively. These data unambiguously suggested the *S* configuration of C-13 [27]. The absolute configuration of C-12 was established by comparing the calculations of OR and $^{13}$C NMR data with these of experimental data [18–21]. The results revealed that the experimental OR value of **8** (+52.0) was similar to the calculated data of **8a**-12*S*,13*S* (+295.6) but was opposite in sign to that of **8b**-12*R*,13*S* (-275.9). Moreover, the higher correlation coefficient and DP4+ probability between the calculated $^{13}$C NMR data of **8a** and the experimental $^{13}$C NMR data of **8** than these between **8b** and **8**. These results suggested that **8a** possessed a better agreement with **8** than **8b** (Fig. 6). The absolute configuration of **8** was thereby confirmed to be 12*S*,13*S*.

(1*R*,5*R*,6*R*,7*R*,10*S*)-1,6-Dihroxyeudesm-4(15)-ene (**11**) had the molecular formula of $C_{15}H_{26}O_2$, deduced from HRESIMS at *m/z* 261.1745 $[M+Na]^+$. The 1D NMR and HSQC spectra exhibited signals for three $sp^3$ methyls, four $sp^3$ methylenes, five $sp^3$ methines [including two oxygenated methines at $\delta_H$ 3.39 (s), and 3.72 (t, $J$ = 9.4 Hz); $\delta_C$ 74.6, and 67.4, respectively], one $sp^3$ quaternary carbon, one $sp^2$ methylenes [$\delta_H$ 5.02 (s), and 4.73 (s); $\delta_C$ 107.1], and one $sp^2$ quaternary carbon [$\delta_C$ 147.9], suggesting that **11** was an analogue of 1*β*-hydroxy-

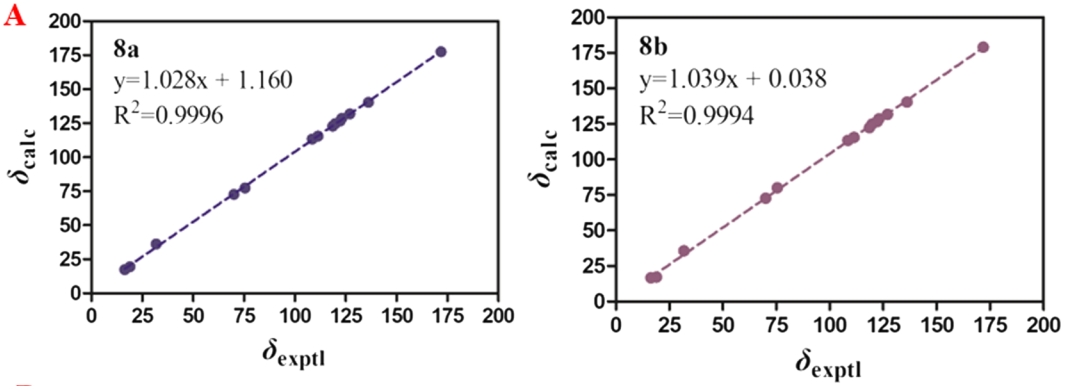


B

| DP+ probability of $^{13}$C NMR of **8** | | |
|---|---|---|
| Plausible isomer | **1a** | **1b** |
| sDP4+ | 89.10% | 10.90% |
| uDP4+ | 44.05% | 55.95% |
| DP4+ | 86.56% | 13.44% |

**Fig. 6.** $^{13}$NMR calculation results of two plausible stereoisomers of **8**. (A) Linear correlation plots of calculated vs experimental $^{13}$C NMR chemical shift values for each potential configuration. (B) The DP4+ probability of the chemical shifts.

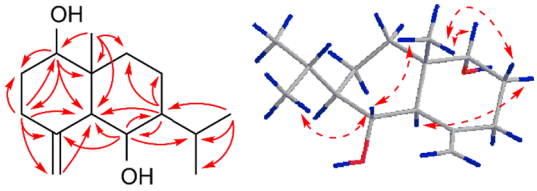


**Fig. 7.** Key HMBC (⟶) and NOESY (⟷) correlations of compound **11**.

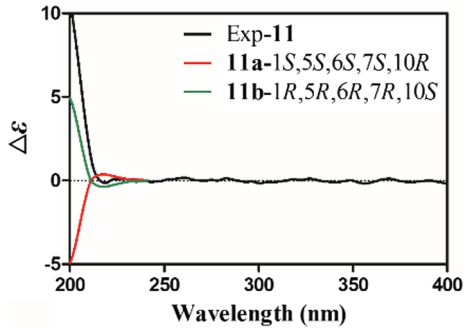


**Fig. 8.** Calculated and experimental ECD spectra of **11a**-(1*R*,5*R*,6*R*,7*R*,10*S*) and **11b**-(1*S*,5*S*,6*S*,7*S*,10*R*).

**Table 2**
Protective Effects of Compounds **1**, **2**, and **7** on PC12 Cell Injury Induced by Glutamate.[a]

| Compound | Cell viability (mean ± SD, %) | | |
|---|---|---|---|
| | 20 μM | 40 μM | 80 μM |
| **1** | 64.7 ± 4.9 | 67.8 ± 5.1 | 72.3 ± 4.5 |
| **2** | 65.9 ± 3.9 | 69.7 ± 2.9 | 74.6 ± 4.0 |
| **7** | 68.4 ± 3.6 | 75.6 ± 4.2 | 84.8 ± 6.5 |

[a] Compounds **3**–**6**, and **8**–**15** were inactive.

6,7*α*-dihy-droxyeudesm-4(15)-ene [28], an eudesmane-type sesquiterpene. Further careful comparison of the 1D NMR data of **11** and those of 1*β*-hydroxy-6,7*α*-dihy-droxyeudesm-4(15)-ene revealed the absence of OH-7 in **11**. The HMBC correlations from H-12 to C-13, C-11, and C-7, and from H-6 to C-4, C-5, C-7, C-11, and C-8 verified the above deduction (Fig. 7).

In the NOESY spectrum, the correlations of Me-12/H-6/Me-15/H-1 and Me-15/$H_a$-2 ($\delta_H$ 1.92) suggested that they were all *α*-oriented, whereas those of $H_b$-2 ($\delta_H$ 1.73)/H-5 revealed the *β*-orientation of H-5. To determine the absolute configuration of **11**, the ECD spectra of **11a**-(1*S*,5*S*,6*S*,7*S*,10*R*) and its enantiomer were calculated. As shown in Fig. 8, the experimental ECD spectrum matched the **11b** data well. Accordingly, the absolute configuration of **11** was finally elucidated as 1*R*,5*R*,6*R*,7*R*,10*S*.

The structures of known compounds were established by comparing their ESI-MS and 1D NMR data with reported data. The compounds were identified as isosclerone (**2**) [29], alternariol methyl ether (**3**) [30], alternariol (**4**) [31], stemphyperylenol (**5**) [32], 1*H*-indole-3-carboxylic acid (**6**) [26], indole-3-methylethanoate (**7**) [26], ergosta-4,6,8(14),22-tetraen-3-one (**9**) [32], (17*R*)-4-hydroxy-17-methylincisterol (**10**) [33], 3(*ζ*)-hydroxy-octadeca-4(*E*),6(*Z*)-dienoic acid (**12**) [34], *E*-7,9-diene-11-methenyl palmitic acid (**13**) [35], *p*-hydroxybenzonic acid (**14**) [36], and benzoic acid (**15**) [37].

### 3.3. Cytotoxicity of compounds 1–15 against four human cancer cell lines

All isolated compounds were evaluated for their cytotoxicity against four cancer cell lines (4T-1, A549, HepG-4, and MCF-7). Among these substances, compound **10** showed cytotoxicity with an $IC_{50}$ value of 9.73 ± 1.2 μM against HepG cells, and **5** exhibited cytotoxicity with $IC_{50}$ values of 4.2 ± 0.6 and 7.9 ± 0.9 μM against MCF-7 and HepG cells, respectively. Other compounds showed no cytotoxic activity on all selected cell lines. Meanwhile, the $IC_{50}$ values of gambogic acid against the 4T-1, A-549, HepG-4, and MCF-7 cell lines were 13.1 ± 1.3, 9.5 ± 1.1, 19.7 ± 2.4, and 15.2 ± 1.5 μM, respectively.

### 3.4. Neuroprotection of compounds 1–15 on injured glutamate induced-PC12 cells

Glutamate, a common endogenous neurotoxin, can cause neuronal cellular necrosis and apoptosis [38]. Therefore, glutamate induced-PC12 cells were used for evaluating the neuroprotective activities of the isolated compounds. Our results showed that the cell viability of the model group and the positive control group were 65.5 ± 5.5% and 92.3 ± 4.6%, respectively. Interestingly, the cell viabilities were significantly improved with the values ranging from 67.8 ± 5.1% to 84.8 ± 6.5 after treatment with compounds **2**, **7** and **9** (40 and 80 μM, respectively) (see Table 2). These results suggested that these three compounds **2**, **7** and **9** possess potential neuroprotective activities.

## 4. Conclusions

In summary, three new compounds (**1**, **8**, and **11**) were isolated from *A. alternate*. Alternin A (**1**) was a novel liphatic polyketone with an unprecedented C25 skeleton. Due to the flexible features of liphatic polyketones, it is quite difficult to establish the absolute configurations of this type of compounds. In this paper, the absolute configuration of **1** was unambiguously determined using the GIAO method. This result will provide a new method for determining the absolute configurations of liphatic polyketones. Moreover, two cytotoxic compounds (**5** and **10**) and three neuroprotective compounds (**2**, **7**, and **9**) were identified in this work.

## Declaration of Competing Interest

All authors declare no conflict of interest.

## Acknowledgement

This research was supported by the National Natural Science Foundation of China (No. 81703382), the China Postdoctoral Science Foundation (2017M621888).

## References

[1] J.C. Wu, Y. Hou, Q.H. Xu, X.J. Jin, Y.X. Chen, J. Fang, B. Hu, Q.X. Wu, ( ± )-Alternamgin, a pair of Enantiomeric Polyketides, from the Endophytic Fungi *Alternaria* sp. MG1, Org. Lett. 21 (2019) 1551–1554.
[2] C.M. Hradil, Y.F. Hallock, J. Clardy, D.S. Kenfield, G. Strobel, Phytotoxins from *Alternaria Cassiae*, Phytochemistry 28 (1) (1989) 73–75.
[3] M.M. Gamboa-Angulo, K. García-Sosa, F. Alejos-González, F. Escalante-Erosa, G. Delgado-Lamas, L.M. Peña-Rodríguez, Tagetolone and tagetenolone: two phytotoxic polyketides from *Alternaria tagetica*, J. Agric. Food Chem. 49 (2001) 1228–1232.
[4] A. Ichihara, H. Tazaki, S. Sakamura, Solanapyrones A, B and C, phytotoxic metabolites from the fungus *Alternaria solani*, Tetrahedron Lett. 24 (48) (1983) 5373–5376.
[5] T. Ueno, T. Nakashima, Y. Hayashi, H. Fukami, Structures of AM-Toxin I and II, host specific phytotoxic metabolites produced by *Alternaria mali*, Agr. BioI. Chern. 39 (5) (1975) 1115–1122.
[6] C.L. Yang, H.M. Wu, C.L. Liu, X. Zhang, Z.K. Guo, Y. Chen, F. Liu, Y. Liang, R.H. Jiao, R.X. Tan, H.M. Ge, Bialternacins A－F, aromatic polyketide dimers from an endophytic *Alternaria* sp, J. Nat. Prod. 82 (4) (2019) 792–797.
[7] J.W. Tang, H.C. Xu, W.G. Wang, K. Hu, Y.F. Zhou, R. Chen, X.N. Li, X. Du, H.D. Sun, P.T. Puno, (+)- and (−)-Alternarilactone A: enantiomers with a diepoxy-cage-like scaffold from an endophytic *Alternaria* sp, J. Nat. Prod. 82 (4) (2019) 735–740.
[8] F.L. Li, W.G. Sun, J.K. Guan, Y.Y. Lu, S.T. Zhang, S. Lin, J.J. Liu, W.X. Gao, J.P. Wang, Z.X. Hu, Y.H. Zhang, Alterbrassicicene A, a highly transformed fusicoccane-derived diterpenoid with potent PPAR-γ agonistic activity from *Alternaria*

*brassicicola*, Org. Lett. 20 (2018) 7982–7986.
[9] Z.X. Hu, W.G. Sun, F.L. Li, J.K. Guan, Y.Y. Lu, J.J. Liu, Y. Tang, G. Du, Y.B. Xue, Z.W. Luo, J.P. Wang, H.C. Zhu, Y.H. Zhang, Fusicoccane-derived diterpenoids from *Alternaria brassicicola*: Investigation of the structure-stability relationship and discovery of an IKKβ inhibitor, Org. Lett. 20 (2018) 5198–5202.
[10] M.Y. Kim, J.H. Sohn, J.S. Ahn, H. Oh, Alternaramide, a cyclic depsipeptide from the marine-derived fungus *Alternar*, J. Nat. Prod. 72 (2009) 2065–2068.
[11] S.X. Cai, J.B. King, L. Du, D.R. Powell, R.H. Cichewicz, Bioactive sulfur-containing sulochrin dimers and other metabolites from an *Alternaria* sp. isolate from a hawaiian soil sample, J. Nat. Prod. 77 (2014) 2280–2287.
[12] Z.Z. Shi, F.P. Miao, S.T. Fang, X.H. Liu, X.L. Yin, N.Y. Ji, Sesteralterin and tricycloalterfurenes A – D: terpenes with rarely occurring frameworks from the marin-alga-epiphytic fungus *Alternaria alternata* k21–1, J. Nat. Prod. 80 (2017) 2524–2529.
[13] G.B. Xu, X. Pu, H.H. Bai, X.Z. Chen, G.Y. Li, A new alternariol glucoside from fungus *Alternaria alternate* cib-137, Nat. Prod. Res. 29 (9) (2015) 848–852.
[14] R.P. Nussbauma, W.G. Ntherb, S. Heinzec, B. Liebermann, New tricycloalternarenes produced by the phytopathogenic fungus *Alternaria alternate*, Phytochemistry 52 (4) (1999) 593–599.
[15] J. Xu, W. Qu, W.Y. Cao, Y. Wang, K.J. Zheng, S.Z. Luo, M.Y. Wu, W.Y. Liu, F. Feng, J. Zhang, Chemical constituents from *Tabernaemontana bufalina* LOUR, Chem. Biodivers. 15 (2019) e1800491.
[16] Spartan 10; Wavefunction, Inc.: Irvine, CA.
[17] M.J. Frisch, G.W. Trucks, H.B. Schlegel, G.E. Scuseria, M.A. Robb, J.R. Cheeseman, G. Scalmani, V. Barone, B. Mennucci, G.A. Petersson, H. Nakatsuji, M. Caricato, X. Li, H.P. Hratchian, A.F. Izmaylov, J. Bloino, G. Zheng, J.L. Sonnenberg, M. Hada, M. Ehara, K. Toyota, R. Fukuda, J. Hasegawa, M. Ishida, T. Nakajima, Y. Honda, O. Kitao, H. Nakai, T. Vreven, J.A. Montgomery Jr., J.E. Peralta, F. Ogliaro, M. Bearpark, J.J. Heyd, E. Brothers, K.N. Kudin, V.N. Staroverov, T. Keith, R. Kobayashi, J. Normand, K. Raghavachari, A. Rendell, J.C. Burant, S.S. Iyengar, J. Tomasi, M. Cossi, N. Rega, J.M. Millam, M. Klene, J.E. Knox, J.B. Cross, V. Bakken, C. Adamo, J. Jaramillo, R. Gomperts, R.E. Stratmann, O. Yazyev, A.J. Austin, R. Cammi, C. Pomelli, J.W. Ochterski, R.L. Martin, K. Morokuma, V.G. Zakrzewski, G.A. Voth, P. Salvador, J.J. Dannenberg, S. Dapprich, A.D. Daniels, O. Farkas, J.B. Foresman, J.V. Ortiz, J. Cioslowski, D.J. Fox, Gaussian 09, Revision C.01, Gaussian, Inc., Wallingford CT, 2010.
[18] J. Xu, H.L. Zhu, J. Zhang, W.Y. Liu, J.G. Luo, K. Pan, W.Y. Cao, Q.R. Bi, F. Feng, W. Qu, Littordials A-E, novel Formyl-phloroglucinol-β-caryophyllene meroterpenoids from the leaves of *Psidium littorale*, Org. Chem. Front. 6 (2019) 1667–1673.
[19] M.W. Lodewyk, M.R. Siebert, D.J. Tantillo, Computational prediction of $^{1}H$ and $^{13}C$ chemical shifts: a useful tool for natural products, mechanistic, and synthetic organic chemistry, Chem. Rev. 112 (2012) 1839–1862.
[20] N. Grimblat, M.M. Zanardi, A.M. Sarotti, Beyond DP4: an Improved probability for the stereochemical assignment of isomeric compounds using quantum chemical calculations of NMR shifts, J. Org. Chem. 80 (2015) 12526–12534.
[21] M.H. Chen, R.Z. Wang, W.L. Zhao, L.Y. Yu, C.H. Zhang, S.S. Chang, Y. Li, T. Zhang, J.G. Xing, M.L. Gan, F. Feng, S.Y. Si, Isocoumarindole A, a chlorinated isocounnarin and indole alkaloid hybrid metabolite from an endolichenic fungus *Aspergillus* sp, Org. Lett. 21 (2019) 1530–1533.
[22] J. Xu, D. Xiao, Q.H. Lin, J.F. He, W.Y. Liu, N. Xie, F. Feng, W. Qu, Cytotoxic tirucallane and apotirucallane triterpenoids from the stems of *Picrasma quassioides*, J. Nat. Prod. 79 (8) (2016) 1899–1910.
[23] J. Xu, H.L. Zhu, J. Zhang, T. Du, E.Y. Guo, W.Y. Liu, J.G. Luo, F. Ye, F. Feng, F. Feng, W. Qu, Sesquiterpenoids from *Chloranthus anhuiensis* with neuroprotective effects in PC12 cells, J. Nat. Prod. 81 (6) (2018) 1391–1398.
[24] T. Mosmann, Rapid colorimetric assay for cellular growth and survival: application to proliferation and cytotoxicity assays, J. Immunol. Methods 65 (1983) 55–63.
[25] D. Takano, T. Nagamitsu, H. Ui, K. Shiomi, Y. Yamaguchi, R. Masuma, I. Kuwajima, S. Omura, Absolute configuration of nafuredin, a new specific NADH-fumarate reductase inhibitor, Tetrahedron Lett. 42 (2001) 3017–3020.
[26] F.Q. Wang, J. Jiang, H.R. Ma, L. Cheng, G. Zhang, Study on secondary metabolites of endophytic *Chaetomium* sp, Chinese Tradit. Herbal Drugs 48 (7) (2017) 1298–1301.
[27] B.N. Su, E.J. Park, Z.H. Mbwambo, B.D. Santarsiero, A.D. Mesecar, H.H.S. Fong, J.M. Pezzuto, A.D. Kinghorn, New chemical constituents of *Euphorbia quinquecostata* and absolute configuration assignment by a convenient mosher ester procedure carried out in NMR tubes, J. Nat. Prod. 65 (2002) 1278–1282.
[28] M.E.F. Hegazy, A.E.H. Mohamed, A.M. El-Halawany, P.C. Djemgou, A.A. Shahat, P.W. Pare, Estrogenic activity of chemical constituents from *Tephrosia candida*, J. Nat. Prod. 74 (5) (2011) 937–942.
[29] J.N. Haruhiro Fujmoto, M.Y. Kentaro Yamaguchi, Immunosuppressive components from an ascomycete, *Diplogelasinospora grovesii*, Chem. Pharm. Bull. 46 (3) (1998) 423–429.
[30] N. Tan, Y.W. Tao, J.H. Pan, S.Y. Wang, F. Xu, Z.G. She, Y.C. Lin, E. Gareth Jones, Isolation, structure elucidation, and mutagenicity of four alternariol derivatives produced by the mangrove endophytic fungus No. 2240, Chem. Nat. Compd. 44 (3) (2008) 296–300.
[31] G.K. Wang, Y. Yu, J.S. Liu, P.L. Zhang, Z.H. Ma, Y.M. Liang, G. Wang, Study on secondary metabolites of endophytic fungus *Alternaria eichhorniae* from *Dendrobium huoshanense*, J. Chinese Med. Mater. 40 (7) (2017) 1614–1617.
[32] H. Fujimoto, E. Nakamura, E. Okuyama, M. Ishibashi, Six Immunosuppressive features from an ascomycete, *Zopfiella longicaudata*, found in a screening study monitored by immunomodulatory activity, Chem. Pharm. Bull. 52 (8) (2004) 1005–1008.
[33] H. Kawagishi, T. Akachi, Chaxine A, an osteoclast-forming suppressing substance, from the mushroom *Agrocybe chaxingu*, Heterocycles 69 (2006) 253–258.
[34] M. Stavri, K.T. Mathew, S. Gibbons, Antimicrobial constituents of *Scrophularia deserti*, Phytochemistry 67 (14) (2006) 1530–1533.
[35] Y.P. Chen, S.L. Wang, Y.H. Shen, Z.J. Wu, Chemical constituents from *Ainsliaea glabra*, Ghuihaia 34 (3) (2014) 402–407.
[36] P.C. Wang, X.L. Zhou, Q. Luo, X. Huang, S.X. Huang, C.M. He, Q. Xu, Chemical constituents from the ethyl acetate parts of the leaves of *Cyclocarya paliurus*, Chin. Pharm. J. 53 (6) (2018) 418–420.
[37] X. Lu, L.L. Zhang, D.Y. Yu, H.G. Wang, L.Y. Shi, L. Tang, Z.X. Yu, B.M. Feng, Chemical constituents in *Urtica angustifolia* Fisch, Central South Pharmacy 13 (12) (2015) 1262–1265.
[38] M. Ankarcrona, J.M. Dypbukt, E. Bonfoco, B. Zhivotovsky, S. Orrenius, S.A. Lipton, P. Nicotera, Glutamate-induced neuronal death: a succession of necrosis or apoptosis depending on mitochondrial function, Neuron 15 (1995) 961–973.